Cofactor Determination and Spectroscopic Characterization of the Selenium-Dependent Purine Hydroxylase from *Clostridium purinolyticum*

William T. Self,‡ Matt D. Wolfe,‡ and Thressa C. Stadtman*

Laboratory of Biochemistry, National Heart, Lung and Blood Institute, National Institutes of Health, 50 South Drive MSC 8012, Bethesda, Maryland 20892-8012

Received June 3, 2003; Revised Manuscript Received July 24, 2003

ABSTRACT: Purine hydroxylase (PH) from *Clostridium purinolyticum* contains a labile selenium cofactor and belongs to a class of enzymes known as the selenium-dependent molybdenum hydroxylases. The presence of approximately 1.1 mol of molybdenum, 0.87 mol of selenium, and 3.3 mol of iron per mol of PH was determined by atomic absorption spectroscopy. Enzyme preparations with lower than stoichiometric amounts of selenium exhibited correspondingly lower hydroxylase activities. Bound FAD, 1 mol per mol enzyme, was confirmed by UV−vis and fluorescence spectroscopy. CMP, released by acid hydrolysis, indicated the presence of a molybdopterin cytosine dinucleotide cofactor. The fully active PH utilized $NADP^+$ as an electron acceptor, and kinetic analysis revealed an optimal k_{cat} of 412 s^{-1} using hypoxanthine as the hydroxylase substrate. Xanthine, NAD^+, and NADPH had no significant effect on this reaction rate. A selenium-independent NADPH oxidase activity was exhibited by native PH. Electron paramagnetic resonance spectroscopy revealed the presence of a Mo(V) desulfo signal, FAD radical, and 2Fe-2S centers in hypoxanthine-reduced PH. No hyperfine coupling of selenium, using ^{77}Se isotope-enriched PH, was observed in any of the EPR active signals studied. The appearance of the desulfo signal suggests that the ligands of Mo in selenium-dependent molybdenum hydroxylases are different from the well-studied mammalian xanthine oxidoreductases (XOR) and aldehyde oxidoreductases (AOR) and suggests a unique role for Se in catalysis.

Molybdenum hydroxylases, a family of enzymes best represented by the well-studied bovine xanthine oxidoreductase (XOR),[1] have been the focus of scientific investigations since the early 1900s (*1*). These metalloenzymes generally contain a similar complement of cofactors: a molybdopterin cofactor, two [2Fe-2S] clusters, and FAD (*2*). Like bovine XOR, most of these enzymes utilize pyridine nucleotide (NAD^+ or $NADP^+$) as an electron acceptor. The molybdenum cofactor has been shown by EPR spectroscopy, X-ray absorption spectroscopy (XAS), and X-ray crystallography to have five ligands: two dithiolene sulfur atoms (part of the molybdopterin cofactor), one oxo ligand, one hydroxyl ligand (which is the source of oxygen during the hydroxylation reaction), and a third sulfur ligand (*2*−*5*). This third sulfur ligand has been termed the cyanolyzable sulfur due to its efficient removal from the enzyme by treatment with cyanide (*6*−*8*). The sulfur atom is required for enzyme activity in all members of the molybdenum hydroxylase family and is a key ligand in the reaction mechanisms proposed for XOR and related hydroxylases (*2*).

A small number of unusual bacterial molybdenum hydroxylases that contain selenium in the form of a labile cofactor have been isolated from *Clostridium sp.* This labile selenium cofactor was first described by Dilworth (*9*) in nicotinic acid hydroxylase (NAH) isolated from *Clostridium barkeri.* Several properties of the enzyme had been characterized in earlier studies on the nicotinic acid fermentation (*10*). Similar enzymes from anaerobic bacteria include xanthine dehydrogenase (XDH) from *Clostridium barkeri* (*11*), *Clostridium purinolyticum* (*12*), *Clostridium acidi-urici*, and *Clostridium cylindrosporum* (*13*). A recent addition to this group of selenoenzymes is purine hydroxylase (PH) from *C. purinolyticum* (*12*). This new member of the class is unique in that it can only hydroxylate the 2- and 6-positions of the purine ring (Figure 1) but is not able to hydroxylate the 8-position (*12*). The labile selenium cofactor present in these enzymes is required for enzyme activity, and in some cases sensitivity to cyanide has been attributed to removal

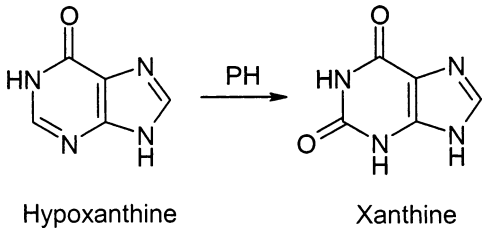

FIGURE 1: Enzyme reaction catalyzed by PH. PH catalyzes the hydroxylation of hypoxanthine to xanthine. This reaction is coupled to the reduction of $NADP^+$ or to other electron acceptors such as DCIP. Unlike numerous XOR enzymes, PH is not able to catalyze the hydroxylation of the 8-position of the purine ring to yield uric acid.

* Corresponding author. E-mail: tcstadtman@nhlbi.nih.gov. Phone: (301) 496-3002. Fax: (301) 496-0599.

‡ These authors contributed equally to this work.

[1] Abbreviations: XOR, xanthine oxidoreductase; AOR, aldehyde oxidoreductase; NAH, nicotinic acid hydroxylase; XDH, xanthine dehydrogenase; PH, purine hydroxylase; MCD, molybdopterin cytosine dinucleotide; FAD, flavin adenine dinucleotide; EPR, electron paramagnetic resonance.

10.1021/bi030136k
Published on Web 09/05/2003

of the selenium (*11*, *12*). In the case of NAH, EPR spectroscopy of a partially oxidized form of the enzyme revealed hyperfine coupling between selenium and the Mo(V) atom (*14*, *15*). Enzyme reduced by added nicotinate did not show hyperfine coupling to Mo(V), indicating that the Se−Mo interaction may be disrupted at some point during catalysis. However, no structural data that might confirm the identity and location of the labile selenium moiety are yet available for NAH or any of the other selenium-dependent hydroxylases.

In the present report, the characterization and quantitation of the cofactors of a highly active and stable PH preparation are described. This enzyme preparation, unlike those described previously that required artificial dyes as an electron acceptor, can utilize $NADP^+$ as an oxidant in hydroxylase reactions with purine substrates. We present the kinetic parameters of the anaerobic hydroxylase reaction with the physiological oxidant as well as the analysis of a selenium-independent NADPH oxidase activity of PH exhibited in the presence of oxygen. Examination of both the hydroxylase and the oxidase reactions in the presence and absence of cyanide strongly suggests that the labile selenium cofactor participates in the early events of the hydroxylation reaction. Although EPR studies indicate that the Se is not structurally analogous to the Mo-bound sulfur atom of other molybdenum hydroxylases, it likely functions in a similar manner.

EXPERIMENTAL PROCEDURES

Growth of C. purinolyticum. C. purinolyticum was cultured as previously described (*12*) with the exception that adenine was the only purine added to the growth medium. Selenium was added in the form of selenite to give a final concentration of 1 μM. This level had been determined to be optimal for maximal expression of active PH (*16*). ^{77}Se (97.2%, Cambridge Isotope Laboratories, Andover, MA)-enriched PH was obtained by growing *C. purinolyticum* in the presence of 1 μM ^{77}Se−selenite prepared as previously described (*14*).

Enzyme Purification. Cells were thawed and washed once with buffer A (100 mM Tricine-KOH, pH 8.0, 0.1 mM PMSF, 0.5 mM EDTA) and ruptured by passage through a French pressure cell at 12 000 psi. The crude cell extract, clarified by centrifugation at 9500*g* for 30 min at 4 °C, was fractionated by stepwise $(NH_4)_2SO_4$ precipitation at 30, 50, and 85% of saturation. The 85% ammonium sulfate pellet that contained PH was resuspended in buffer B (buffer A lacking PMSF) containing 1 M $(NH_4)_2SO_4$ and applied to a phenyl-Sepharose column (Pharmacia, Uppsala, Sweden) equilibrated with the same buffer. PH was eluted with a gradient of 1.0−0 M $(NH_4)_2SO_4$ in buffer B, and the PH-containing fractions were pooled and adjusted to 1 M $(NH_4)_2SO_4$. This enzyme solution was applied to a butyl-Sepharose column (Pharmacia, Uppsala, Sweden) and eluted with a similar gradient of $(NH_4)_2SO_4$. PH-containing fractions were pooled, dialyzed overnight against buffer B, and applied to a DEAE column. A gradient of 0−0.5 M KCl in buffer B was utilized to elute PH from this column, and PH-containing fractions were pooled and concentrated using Centriprep 15 concentrators (Amicon, Bedford, MA). This fraction was loaded onto a S-300 gel filtration column (Pharmacia, Uppsala, Sweden), and buffer B containing 0.29 M KCl was applied. Fractions containing significant PH activity were pooled, diluted 2-fold in buffer B to reduce the KCl concentration, and again loaded onto a DEAE column. Using a gradient of 0−0.3 M sodium citrate for elution, a final separation of PH from contaminating proteins was achieved. The homogeneous PH pool was dialyzed overnight against 100 mM Tricine-KOH, pH 8.0 containing 0.25 M $(NH_4)_2SO_4$.

Enzyme Assays. PH activity was measured by following NADPH production in sodium phosphate buffer (0.1 M, pH 7.75) with hypoxanthine as substrate, unless otherwise noted. A solution containing buffer, PH, and 1 mM $NADP^+$ was exhaustively degassed by sparging with Ar or N_2 prior to the addition of substrate (also under Ar or N_2) to 1 mM to start the reaction. The initial rate of reduction of $NADP^+$ was followed by measuring absorbance increases at 340 nm. In adenine inhibition studies, the hydroxylase reaction was started by the addition of appropriate substrate within 1 min after the addition of adenine. NADPH oxidase assays were performed under aerobic conditions as previously described for nicotinic acid hydroxylase (*15*). All assays were performed at 25 °C, and kinetic constants were derived from fits to double reciprocal plots. Cyanide treatment of PH was carried out in a Coy anaerobic chamber (Grass Lake, MI) using KCN essentially as previously described (*7*, *8*, *12*). PH activity was assayed at various time points to determine the extent of inactivation by KCN during treatment.

Determination of Cofactor Composition. Selenium, molybdenum, and iron were determined using a Perkin-Elmer 4100 ZL atomic absorption spectrometer with Zeeman background correction. PH was diluted in 1% nitric acid prior to analysis. Labile flavin was released from PH by heating at 100 °C for 5 min and separated by centrifugation at 18 500*g* for 15 min. Flavin was isolated by HPLC using a C_{18} column as previously described (*17*). Both UV and fluorescence spectroscopic techniques confirmed the presence of FAD in the cofactor solution after heat treatment. The amount of FAD per mol of PH was determined by calculating the difference in the absorbance of the native PH at 450 nm before and after reduction with dithionite, using $\epsilon_{450} = 11\,500$ for oxidized FAD and $\epsilon_{450} = 980$ for reduced FAD. Nucleotide content was determined after acid hydrolysis and HPLC analysis of nucleotides as previously described (*18*).

Spectroscopic Methods. All EPR samples were prepared in the Coy anaerobic chamber maintained at <5 ppm O_2. Each sample was incubated for 10 min at room temperature after the addition of substrate and subsequently frozen and stored in liquid nitrogen. High temperature (120 K) X-band EPR spectra were recorded on a Bruker ESP-300S EPR spectrometer. Low temperature (<40 K) spectra were recorded on either a Bruker E500 or Bruker E580 spectrometer, each equipped with and ESR-910 liquid helium cryostat (Oxford Instruments). All spectra were collected in perpendicular mode using a Bruker 4102ST resonator. Spin quantification was performed by measuring spectra under nonsaturating conditions and using a 1 mM Cu(II)-EDTA standard as described (*19*). All spectral manipulations and simulations were performed using the WINEPR software package provided by Bruker. PH samples prepared for optical absorption spectroscopy were identical to those used for EPR experiments and were sealed throughout the experiment to prevent oxidation of the reduced enzyme by oxygen. All optical spectra of PH and enzyme activities were measured

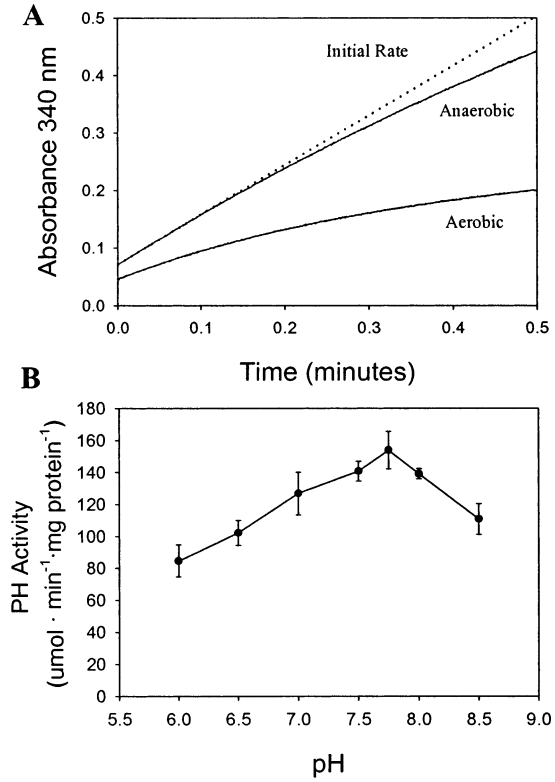

FIGURE 2: Optimization of PH activity. (A) The hypoxanthine-dependent reduction of $NADP^+$ catalyzed by purine hydroxylase. Production of NADPH is monitored at 340 nm. (B) Determination of pH optimum for PH activity using hypoxanthine as substrate and $NADP^+$ as electron acceptor. The initial rate of reduction of $NADP^+$ in a phosphate-buffered system is plotted vs pH. Points represent the mean of at least three independent determinations, and error bars represent one standard deviation above and below this mean.

using a Cary 100 UV−vis spectrophotometer (Varian Analytical Instruments, Walnut Creek, CA).

RESULTS

Fully Active Purine Hydroxylase Reduces $NADP^+$. Purine hydroxylase originally was detected during the purification of xanthine dehydrogenase, another selenium-dependent molybdoenzyme present in *C. purinolyticum*. Subsequent preparations of PH exhibited significant increases in enzyme activity when a higher ionic strength was maintained during the purification procedure. These more active preparations could reduce pyridine nucleotides, and $NADP^+$ was shown to be a preferred and efficient electron acceptor.

Figure 2 illustrates the hypoxanthine-dependent reduction of $NADP^+$ by PH. In air-saturated buffer, there is an initial reduction of $NADP^+$, but the rate of conversion of $NADP^+$ to NADPH rapidly decreases. Attempts to recover activity by the addition of more substrate or by gel filtration or dialysis of the enzyme to remove potentially bound inhibitory products were unsuccessful. Under anaerobic conditions, the rate of reduction of $NADP^+$ is linear early in the reaction (first 10−15 s) but decreases over time, although at a lower rate than in the presence of oxygen. Inactivation of PH was observed even under rigorously anaerobic conditions when assayed in the NIH Building 3 anaerobic chamber (*20*). In this case, oxygen had been removed for several hours from all components of the reaction mixture; thus, inactivation was not due to a small residual oxygen contamination. Similar inactivation of enzyme during the assay procedure also was observed with enzyme derived from *C. purinolyticum* cells ruptured by sonication in the anaerobic chamber and protected during subsequent steps from contact with an oxidizing environment. The nature of the inactivation of PH during turnover is still unknown. Therefore, in the present study, all PH activities reported are based on the initial linear rate of reduction of $NADP^+$ under anaerobic conditions.

Table 1: Kinetic Parameters of PH Using NADP as an Electron Acceptor

substrate	K_m (μM)	k_{cat} (s^{-1})	k_{cat}/K_m ($M^{-1}\,s^{-1}$)
hydroxylation reaction			
purine	21.3	133	6.2×10^6
hypoxanthine	33.9	412	1.2×10^7
2OH-purine	117.0	146	1.3×10^6
NADP	26.0	N/A	N/A
NADPH oxidase			
NADPH	50.5	78	1.5×10^6

Determination of Kinetic Constants for Purine Substrates Using $NADP^+$ as an Electron Acceptor. The pH optimum for catalytic activity of purine hydroxylase with 1 mM hypoxanthine and 1 mM $NADP^+$ as substrates was determined using various monobasic and dibasic sodium phosphate buffers at 0.1 M concentration (Figure 2B). The 1 mM concentrations of hypoxanthine and $NADP^+$ were determined to be saturating (see below). At the determined optimum pH of 7.75, no increase in enzyme activity was observed upon changing ionic strength. The calculated specific activity using hypoxanthine as substrate under optimized conditions was 167.9 μmol min^{-1} mg^{-1} (from Michaelis−Menten plots, data not shown), which corresponds to a k_{cat} of 412 s^{-1} (Table 1). This is a significant increase over the previously reported activity of previous preparations using DCIP as an electron acceptor (k_{cat} = 5 s^{-1}, ref *12*). The optimized activity is similar to that of XDH from *C. barkeri* (reported as a specific activity of 164 μmol min^{-1} mg^{-1} protein, or approximately 400 s^{-1}), an enzyme that also has been reported to contain a labile selenium cofactor.

Table 1 lists the kinetic constants K_m and k_{cat} for PH with several purines as substrates and $NADP^+$ as the electron acceptor. Although the K_m for purine is lower than for hypoxanthine, the k_{cat} is also significantly lower than that obtained for hypoxanthine resulting in a lower specificity constant. The most efficient substrate, hypoxanthine (6-OH-purine), is generally accepted as the actual physiological substrate since growth of *C. purinolyticum* depends on the addition of adenine to the medium (*21*), and the adenine deaminase present in the organism would produce hypoxanthine from the adenine (*22*). On the other hand, 2-OH-purine, which also yields xanthine upon hydroxylation by PH (*12*), has a lower k_{cat}, and based on its higher K_m value, presumably is bound less efficiently than hypoxanthine.

PH Exhibits NADPH Oxidase Activity. Many FAD-containing enzymes catalyze the oxidation of reduced pyridine nucleotides in the presence of oxygen, termed NAD(P)H oxidase. PH exhibits NAD(P)H oxidase activity and preferred NADPH over NADH. The NADPH oxidase activity was not significantly inhibited by $NADP^+$, NAD^+, or NADH (data not shown). In phosphate buffers, the NADPH oxidase

activity increased over the entire pH range from 6.5 to 9.0. In buffers above pH 9.0, the highest NADPH oxidase activity observed was at pH 11.0 in 0.1 M CAPS buffer. Above pH 11.0, the activity fell rapidly. Even at this high pH, NADPH oxidase activity obeyed Michaelis−Menten kinetics and yielded a k_{cat} of 78 s^{-1} and a K_m for NADPH of 50.5 μM (Table 1). Preincubation of PH with KCN to inhibit purine hydroxylation activity (*12*) had no significant effect on NADPH oxidase activity (measured at pH 7.75, data not shown). Similarly, the selenium-dependent hydroxylase, NAH, has been reported to have NADPH oxidase activity that is not dependent on selenium (*14*).

Inhibition Studies of PH. $NADP^+$ is the preferred electron acceptor in the hydroxylase reaction, and NAD^+ serves as an electron acceptor for PH but at a much reduced rate (12 s^{-1}). However, addition of NAD^+, NADH, or NADPH in concentrations up to 0.5 mM had no significant effect on the rate of reduction of $NADP^+$ by PH with hypoxanthine as substrate. Xanthine, the product of hypoxanthine hydroxylation, had no effect on the rate of $NADP^+$ reduction when added in concentrations up to 5 mM (data not shown). Although the products of the reaction, NADPH and xanthine, do not inhibit hypoxanthine hydroxylation, a survey of other available purines revealed significant inhibition in the presence of adenine.

The type of inhibition caused by adenine was examined using either purine or hypoxanthine as substrate while varying the concentrations of both substrate and adenine, and the results of these studies are shown in double reciprocal plots (Figure 3A,B). Both plots suggest that adenine behaves as a noncompetitive inhibitor of the hydroxylation reaction. Plots of the slopes of the double reciprocal plots against adenine concentration gave an approximate K_i value of 0.9 mM for both substrates (Figure 3, inset plots). Adenine showed no inhibitory effect on the PH NADPH oxidase activity. Since adenine has an available site for hydroxylation by PH at the 2-position, and this site is known to be hydroxylated when hypoxanthine is incubated with PH (*12*), further investigation into the inhibitory effect of adenine utilized spectroscopic techniques.

Noncompetitive inhibition of PH by adenine suggested that adenine binds at a site other than the substrate site or to a different form of PH than substrate. To determine if adenine is able to reduce any of the redox active sites of PH, the absorption spectrum of anaerobic PH in the presence of adenine was compared to the spectrum of the enzyme reduced anaerobically by hypoxanthine in the absence of oxidant. Figure 4 shows the UV−vis absorption spectrum of PH as isolated (solid line). This spectrum is similar to those of other molybdenum hydroxylases that contain oxidized flavin and FeS cofactors. After a 10 min incubation with hypoxanthine, a loss of absorption is observed in the 350−460 nm range accompanied by an increase in absorption from 550 to 750 nm (Figure 4, dotted line). The observed change in the optical spectrum is consistent with flavin reduction to a neutral semiquinone state. Further evidence for formation of the semiquinone and reduction of FeS clusters is described later. Similarly, incubation of PH with adenine for 10 min resulted in reduction of the enzyme, although to a lesser extent. These data prompted a reevaluation of adenine as an actual substrate for PH. At higher enzyme concentrations, adenine indeed functions as a

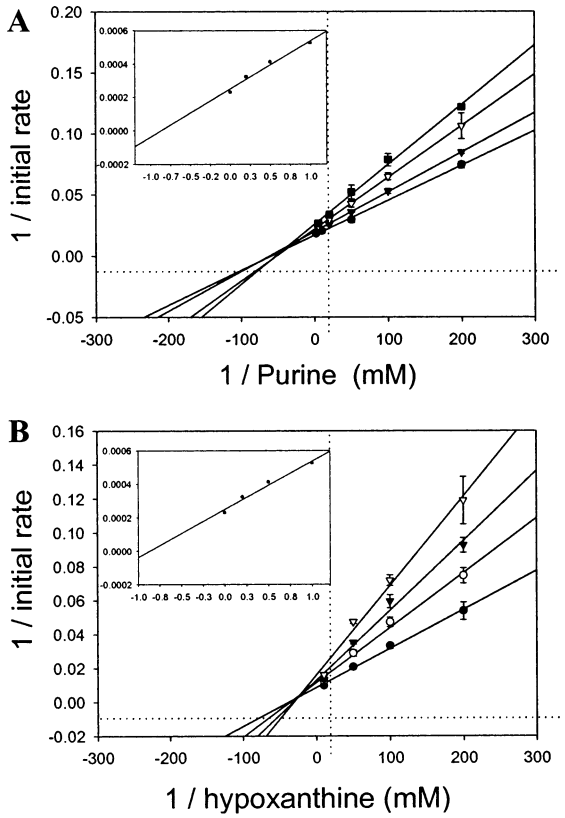

FIGURE 3: Kinetic plots examining adenine inhibition of PH. Double reciprocal plots of adenine inhibition of PH hydroxylase activity using $NADP^+$ as the oxidant and either purine (A) or hypoxanthine (B) as the hydroxylase substrate. The slopes from the double reciprocal plots are plotted against the adenine concentration to obtain the inhibition constant K_i and are shown in the inset graphs.

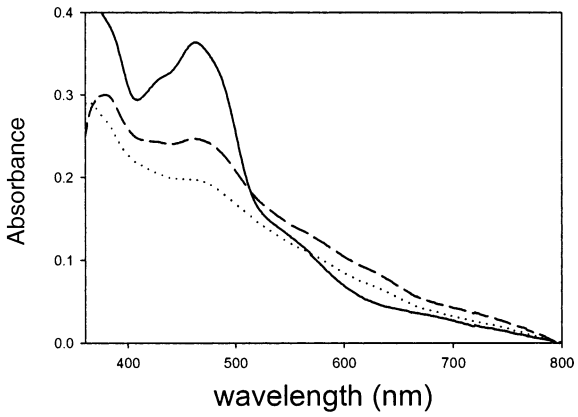

FIGURE 4: Optical absorption spectra of PH in the presence of hypoxanthine and adenine. Isolated PH (solid line) was incubated under anaerobic conditions with either 5 mM hypoxanthine (dotted line) or adenine (dashed line).

substrate for PH, albeit at a far lower turnover rate than with hypoxanthine. A specific activity of 0.64 μmol min^{-1} mg^{-1} was obtained using 5 mM adenine as substrate and $NADP^+$ as the electron acceptor, about 0.3% of the activity obtained using hypoxanthine. It is assumed that the product of this hydroxylation of adenine is 6-amino-2-hydroxy-purine, although this has not been established. These results demonstrate that, although adenine behaves as a noncompetitive inhibitor of hypoxanthine and purine-dependent reduction of $NADP^+$, it is in fact a substrate with a very slow rate of

Table 2: Cofactor Content and Metal Analysis of PH

cofactor/metal	mol/mol enzyme	method of determination
molybdenum	1.1 ± 0.11	AAS[a]
iron	3.3 ± 0.33	AAS
selenium	0.87 ± 0.10	AAS
FAD	1.1	UV−vis spectrometry/HPLC

[a] AAS—atomic absorption spectroscopy.

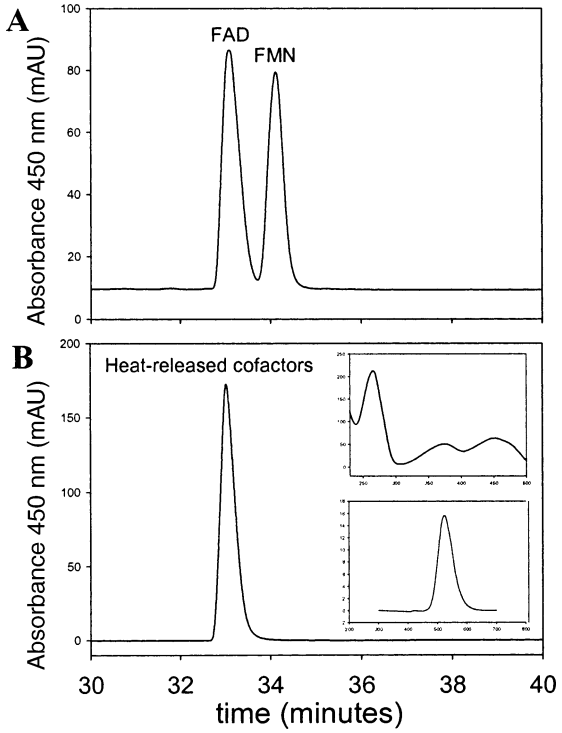

FIGURE 5: Determination of the flavin component of PH. HPLC separation of the heat-released components of PH. Details of the chromatographic conditions are in the Experimental Procedures. (A) UV absorption at 450 nm vs elution time of a reference solution of FAD and FMN. (B) UV absorption at 450 nm vs elution time of the heat stable component derived from PH. Both the UV-vis spectrum (upper) and fluorescence emission spectrum (lower) of the 33 min peak are shown in the inset graphs.

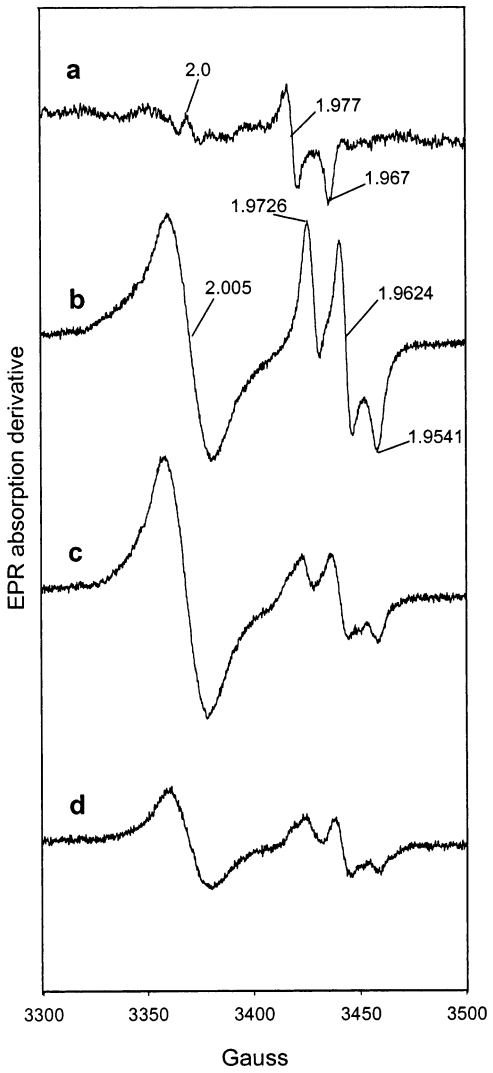

FIGURE 6: EPR spectra of PH at 120 K. As isolated PH (spectrum a) or reduced with hypoxanthine (spectrum b), adenine (spectrum c), or NADPH (spectrum d) each at 5 mM. The spectrum in part a is the result of 10 consecutive summed scans. Instrument conditions: microwave power, 2 mW; modulation amplitude, 5 G; microwave frequency, 9.45 GHz.

turnover. By taking advantage of this slow turnover, adenine may prove to be useful in future studies to address the overall enzyme mechanics of PH.

Determination of PH Cofactor Composition. On the basis of the previously determined molecular weight of 147 500 Da of PH (*12*), AAS analysis of PH revealed a stoichiometric concentration of molybdenum per mol of enzyme (Table 2). Selenium also was present in a near stoichiometric amount, at 0.87 mol per mol of PH. Although the amount of selenium varies from preparation to preparation, the specific activity correlates with the selenium content (data not shown). Similar results were reported for the AAS analysis of selenium contents for NAH (*15*). An iron content of 3.3 mol per mol of enzyme suggests that PH does contain FeS centers, as expected for an enzyme of the molybdenum hydroxylase family.

Flavin was identified as FAD by HPLC−UV−fluorescence determination (Figure 5). Acid hydrolysis of PH revealed both AMP (derived from FAD) and CMP. The equimolar presence of CMP (1.15 mol/mol AMP) indicates that the molybdenum cofactor present in PH is molybdopterin cytosine dinucleotide (MCD). Table 2 summarizes the cofactor content determined for PH.

EPR Analysis of PH Cofactors. All molybdenum hydroxylases contain redox active cofactors that cycle through different oxidation states during turnover. Several of these states are paramagnetic and are observable using EPR spectroscopy. We used EPR spectroscopy to study the PH cofactors at both high (120 K) and low (20 K) temperatures. As isolated, PH has only weak features in the X-band EPR spectrum measured at 120 K (Figure 6, spectrum a). A single anisotropic species is observed with *g*-values of 2.0, 1.977, and 1.967, which we assign to a minor Mo(V) $S = {}^1/_2$ component (<0.1 spin/PH) indicating that the majority of the molybdenum present in the sample is in either the oxidized Mo(VI), or less likely, reduced Mo(IV) oxidation state. At this temperature, FAD reduced to the semiquinone state would likely be observed. However, no significant radical signal is seen indicating the presence of oxidized flavin, consistent with the optical spectrum of PH as isolated (see Figure 4).

Addition of hypoxanthine to PH in the absence of an electron acceptor, under anaerobic conditions, results in reduction of the enzyme (Figure 4). Figure 6, spectrum b shows the appearance of two major species in the EPR spectrum of this sample measured at 120 K. First, an isotropic $S = {}^1/_2$ signal is seen at $g \sim 2$ (1 spin/PH, line width = 21 G), characteristic of a flavin semiquinone radical (*2*). Second, an anisotropic species is seen in the spectrum with *g*-values of 1.973, 1.962, and 1.954, consistent with an $S = {}^1/_2$ Mo-(V) center in PH. This species, however, is different than that observed in PH as isolated and accounts for the majority of the Mo in the reduced sample (>0.5 spin/PH). Similar spectra were obtained when PH was reduced with the alternative substrate adenine (Figure 6, spectrum c) or NADPH (Figure 6, spectrum d). However, the extent of FAD and Mo reduction varied between reduction methods when incubated for the same period of time. While adenine reduction of the Mo center was expected, we anticipated only observing reduced FAD upon reduction with NADPH, as was observed with NAH (*15*). However, it appears that reduction in the reverse direction leads to distribution of electrons throughout the electron-transfer pathway, including FeS clusters (see below).

To observe faster relaxing species such as FeS clusters, EPR spectra were recorded at 20 K. Figure 7, spectrum a shows the spectrum of PH as isolated in which no signals are observed. However, after reduction with hypoxanthine, a complex spectrum is produced indicating that several paramagnetic species are present (Figure 7b). Through the use of power saturation studies, we were able to deconvolute the spectrum into four different $S = {}^1/_2$ species: a Mo(V) center, two distinct FeS clusters, and a broad FAD semiquinone radical. Figure 7, spectra c−f show the results of the respective simulations using the parameters listed in Table 3. The Mo(V) signal and FAD semiquinone represent the paramagnetic centers also seen at the high temperature described above. The two FeS signals seen at 20 K are assigned as reduced [2Fe-2S] centers in which an Fe(III) and Fe(II) anitferromagnetically couple to yield $S = {}^1/_2$ systems. The observation of two [2Fe-2S] clusters is common in molybdenum hydroxylase enzymes, and the uniquely broad spectrum of one of the clusters is seen in several molybdoenzymes (ref *24* and references therein). By convention, we assign the unusually broad cluster having *g*-values of 2.080, 1.968, and 1.907 as [2Fe-2S]II and the other cluster [2Fe-2S]I (*24*). Figure 7, spectrum g shows the simulated composite spectrum following adjustment for each species' concentration. All species were present in concentrations compatible with cofactor concentrations determined by independent techniques (>0.6 spin/PH, see above) with the exception of Mo, which is saturated under the experimental condition.

Low temperature EPR spectra were also collected for samples reduced by adenine and NADPH. These spectra, like those collected at the higher temperature of 120 K, were nearly identical in line shape to the PH sample reduced with hypoxanthine for the same period of time (data not shown). However, the total intensity of paramagnetic species and differences in relative population of the Mo(V), flavin semiquinone, and FeS clusters were observed. It appears that regardless of the method of reduction, reducing equivalents are distributed throughout the reducible centers suggesting

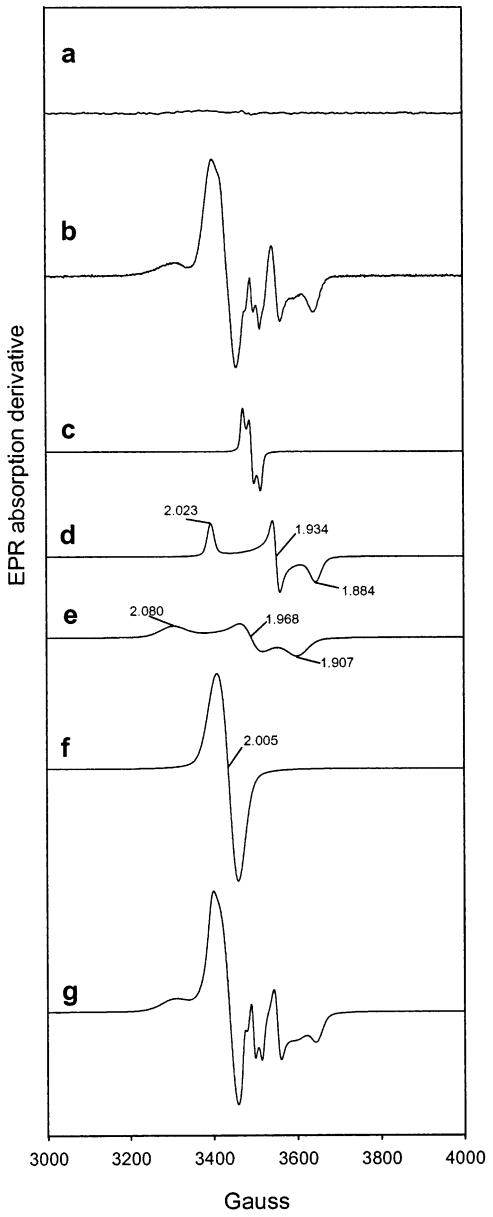

FIGURE 7: EPR spectra of PH at 20 K. As isolated PH (spectrum a) or reduced with (spectrum b) hypoxanthine (5 mM). Spectra in parts c−g are simulations using values listed in Table 3, and part g is the resulting spectrum from the combined simulations (spectra c−g). Instrument conditions: microwave power, 200 μW (spectra a and b); modulation amplitude, 5 G; microwave frequency, 9.61 Ghz.

Table 3: EPR Parameters of PH

g-value (line width, in G)	g_1	g_2	g_3
120 K			
Mo(V)	1.9726(4.6)	1.9624(4.6)	1.9541(5.5)
FAD radical		2.005(21.2)	
20 K			
[2Fe-2S]I	2.023(15)	1.934(13)	1.884(25)
[2Fe-2S]II	2.080(57)	1.968(40)	1.907(45)

that under the experimental condition, the redox potential of the centers are similar. However, it must be pointed out that in the experiments described above, all PH samples were incubated with reductant for the same period of time (10 min). Therefore, equilibrium conditions for each of the reducing agents may not have been established, leading to

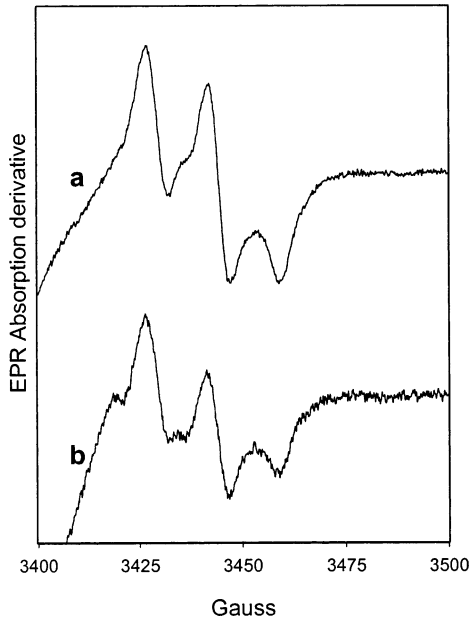

FIGURE 8: Comparison of the Mo(V) EPR spectra of natural abundance and ^{77}Se-enriched PH. PH isolated from *C. purinolyticum* cultured in natural abundance Se (spectrum a) and 97% ^{77}Se (spectrum b). Spectrum b has been multiplied by a factor of 2 due to a lower Se concentration in the sample. Instrument conditions: microwave power, 20 mW; modulation amplitude, 5 G; microwave frequency, 9.46 GHz.

the variability in both the extent of reduction and the extent of distribution of reducing equivalents. Future experiments using poised potentials under equilibrium conditions will be used to estimate actual redox potentials of the individual PH cofactors.

Nature of the Selenium in PH. Selenium present in PH, approximately 1 mol of Se/mol of enzyme, is required for hydroxylase activity of the enzyme. By analogy to the cyanolyzable sulfur bound to the Mo in other hydroxylases, the Se may directly interact with the Mo center in PH, as has been previously inferred in selenium-dependent NAH (*15*). To detect coordination of selenium and molybdenum in PH, the enzyme was purified from cells grown on ^{77}Se ($I = {}^1/_2$), and EPR spectra were collected. Figure 8 shows a 120 K spectral comparison between hypoxanthine-reduced PH containing natural abundance Se (Figure 8, spectrum a) and ^{77}Se-enriched PH (Figure 8, spectrum b). Clearly, no hyperfine coupling between the Mo(V) center and the Se nucleus is observed in either sample. Broadening of the resonances could not be detected either, for simulations of spectra of both the natural abundance and the ^{77}Se-enriched samples gave identical line widths. For completeness, we looked for hyperfine coupling between the Se nucleus and the FAD semiquinone of the reduced sample, and Se and Mo of PH as isolated, but no interaction was observed (data not shown). Low temperature EPR spectra also were recorded for reduced PH enriched with ^{77}Se. However, no differences were observed between enriched and unenriched samples indicating that no detectable coupling between the Se nucleus and the paramagnetic FeS clusters of reduced PH occurs.

The above data indicate that either there is no Mo−Se interaction or it cannot be resolved under the experimental conditions used. To address these possibilities, we treated PH with KCN (30 mM final concentration) for 6 h (<5% catalytic activity remaining) and again measured the EPR

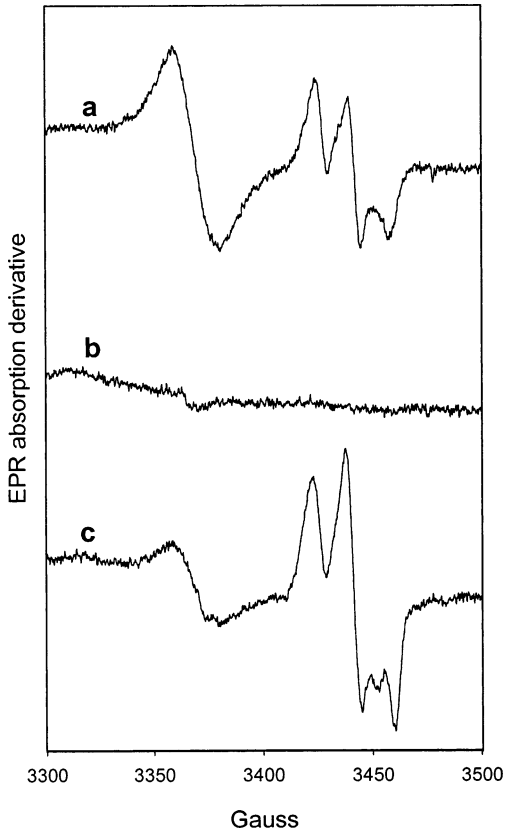

FIGURE 9: EPR spectra of cyanide inhibited PH. Hypoxanthine reduced PH without cyanide treatment (spectrum a) or after treatment with 30 mM cyanide for 6 h (spectrum b). Part c as in part b but after treatment with 5 mM NADPH. Instrument conditions: microwave power, 20 mW; modulation amplitude, 5 G; microwave frequency, 9.46 GHz.

spectrum of the Mo center after the addition of hypoxanthine. This KCN treatment results in a loss of Se (as determined by subsequent gel filtration and atomic absorption spectroscopy, data not shown). Figure 9 shows the 120 K spectra of both untreated (spectrum a) and cyanide-inhibited (spectrum b) PH, each in the presence of added hypoxanthine and in the absence of external oxidant. It is apparent that while the untreated sample shows typical Mo(V) and flavin radical signals, these are not detected in the KCN-treated sample. Similarly, no reduced FeS clusters were present in the low temperature EPR spectrum of the KCN-treated sample (data not shown). From these results, we conclude that the cyanide treatment inactivates the enzyme such that reduction by hypoxanthine is prevented.

The mechanism of KCN inactivation of the enzyme could involve cyanolysis of the selenium cofactor present as a perselenide derivative (of cysteine) or a molybdenum-bound selenium atom but may also target other redox active centers in PH. To address these possibilities, we took advantage of the fact that PH can be reduced in the reverse direction by NADPH. Figure 9, spectrum c shows the 120 K spectrum of KCN-treated PH (in the presence of hypoxanthine) following treatment with NADPH (5 mM, 10 min). Clearly, Mo(V) and flavin semiquinone are observed, indicating successful reduction of PH via the FAD and FeS cluster sites. The low temperature EPR spectrum of this sample also revealed reduced FeS clusters only after the addition of NADPH (data not shown). Thus, the cyanolyzable Se appears to be involved in the early steps of catalysis, likely at the

Mo center, and not in the electron transfer events between FeS clusters and FAD. On the basis of data that provide no evidence of a direct interaction between Se and the Mo cofactor or any significant perturbation at the Mo center upon Se removal, it seems unlikely that cyanide inhibition can be attributed solely to the disturbance of a direct coordination of Se to the Mo center and strongly suggests that the selenium is present in the form of a perselenide near the Mo atom.

DISCUSSION

The catalytic activity of PH utilized in this study was more than 50-fold greater than in previous preparations. This is likely due to improved stability of the enzyme and the use of $NADP^+$ as the electron acceptor under optimized conditions. In the reaction with purine, the 6-position is attacked first, followed by a reaction at position 2 to yield xanthine as the final reaction product. The inability of PH to hydroxylate xanthine makes it a unique member of the XOR-like enzymes. However, from a physiological standpoint this inability to convert xanthine further to uric acid is logical because in the purine fermentation pathway of purinolytic *Clostridia*, xanthine production is the point at which ring cleavage occurs (*24*). Other purine substrates such as adenine must first be modified before being channeled into the xanthine cleavage pathway. Adenine, after conversion to hypoxanthine by adenine deaminase, can then be hydroxylated to xanthine by PH. Therefore, it is not surprising that adenine per se is ineffective as a substrate for PH despite it being structurally analogous to hypoxanthine. Studies in which adenine was treated as an inhibitor of the PH reaction revealed that it acts as a mixed-type, noncompetitive inhibitor with respect to purine or hypoxanthine. This result indicates that in addition to being a poor hydroxylase substrate, adenine can bind to a different form of PH in addition to that which binds purine and hypoxanthine. However, a more thorough kinetic investigation is required to determine at which points in the PH catalytic cycle adenine exerts its inhibition effects.

In the course of our investigations of PH function, we found that the enzyme, like many other flavin-containing oxidoreductases including XOR, exhibits significant NADPH oxidase activity. Presumably, after reduction by NADPH and subsequent oxidation by molecular oxygen, one or more of the reduced PH cofactors undergoes oxidation. We utilized the ability to reduce PH by NADPH in the back reaction as part of our kinetic and spectroscopic studies. In the case of adenine inhibition, no inhibitory effect on the NADPH oxidase activity is observed, ruling out adenine interactions at the site of $NADP^+$/NADPH binding as a cause of the mixed-type inhibition pattern. Removal of selenium from PH by cyanide treatment had no effect on the NADPH oxidase activity indicating that Se does not participate in electron transfer at the flavin site. Thus, it is unlikely that Se plays a role in flavin oxidation/reduction during the hydroxylase reaction.

Like other members of the molybdenum hydroxylase family, PH contains a stoichiometric amount of Mo, FAD, and FeS clusters. In addition, PH contains 1 mol of selenium, which is the defining characteristic of these selenium-dependent molybdenum hydroxylases. Flavin analysis, UV/vis, and variable temperature EPR spectroscopy indicate that the FAD component of PH exists as a one-electron reduced neutral blue semiquinone in the reduced enzyme. In addition, EPR spectroscopy of reduced PH indicates the presence of two [2Fe-2S] clusters, [2Fe-2S]I and [2Fe-2S]II, and a Mo(V) center. Upon reduction of the enzyme, our studies indicate that all cofactors are reduced, making the analysis of relaxation processes of a reduced center in the presence and absence of other reduced centers difficult. Thus, we could not gain structural information about PH by determining if one or more of the paramagnetic centers magnetically interacts with a neighboring cofactor. In a recent analysis of signals I and II from a variety of molybdoenzymes, Caldeira et al. show the 2Fe-2S cluster yielding signal I is that closest to the Mo active sites in xanthine oxidase and *Desulfovibrio gigas* aldehyde oxidoreductase (*23*). On the basis of these studies, we have assigned the FeS cluster with a broader signal (Figure 7, spectrum f) as the cluster that lies closest to the Mo center, although this assignment will need to be confirmed in future analysis of the redox potentials of each of the redox active sites in PH.

The molybdopterin cofactor in PH occurs as a molybdopterin cytosine dinucleotide, based on the presence of CMP in an acid hydrolysate. We studied the Mo center using EPR spectroscopy and found that PH as isolated contains a small fraction of Mo(V), with the balance of Mo centers likely being in the (VI) oxidation state. Upon reduction of PH with hypoxanthine, a nearly stoichiometric amount of Mo(V) is observed consistent with substrate reduction of the cofactor. However, the 120 K EPR spectrum of the Mo(V) center of PH is quite unusual in that it closely resembles spectra of desulfo forms of other molybdenum hydroxylases prepared by cyanolysis of the Mo−S bond in these enzymes. This would suggest that the cyanolyzable sulfur, which is well-described and required for activity in molybdenum hydroxylase enzymes, may not be present in the *Clostridial* enzymes. Another member of the selenium-dependent hydroxylase family, XDH from *C. acidiurici*, was also shown to exhibit a desulfo Mo(V) EPR signal upon reduction. These observations indicate that the active forms of the *Clostridial* enzymes likely contain a Mo center with different properties than typical molybdenum hydroxylases. This may also explain why the hydroxylases from *Clostridia* (and other obligate anaerobes) uniquely contain a labile selenium cofactor.

We considered that the labile Se is bound to the Mo center analogous to the cyanolyzable thiolene in typical molybdenum hydroxylases. Such an interaction would likely be observed as hyperfine coupling in the EPR spectrum of ^{77}-Se-enriched PH. Indeed, this method has revealed an interaction between Se and Mo(V) in partially oxidized NAH as well as reduced formate dehydrogenase (FDH) from *Escherichia coli*. In the case of FDH, the selenium is covalently bound to the enzyme as selenocysteine that serves as a ligand to the active site molybdenum. However, our studies on PH reported here show no evidence of a Mo−Se interaction in either the as-isolated or substrate-reduced state, suggesting that either the Se is not bound to the Mo center or the Mo−Se interaction is simply not detectable by EPR spectroscopy. While we cannot rule out the latter possibility, it seems unlikely that Se interacts directly with Mo since cyanide treatment followed by reduction of PH with NADPH produces a Mo(V) center nearly spectroscopically identical to untreated, reduced PH.

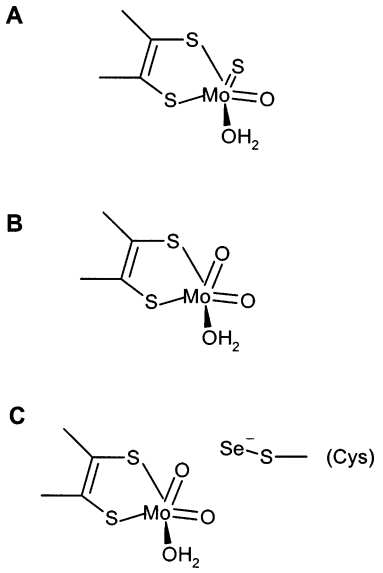

FIGURE 10: Active sites of molybdenum hydroxylases. The molybdenum coordination environment of active XOR (A) and desulfo XOR (B) are based on the reported structures of Mop (*26*) and on the cumulative evidence presented for XOR in ref *2*. Also shown is our proposed structure of the active site of the selenium-dependent purine hydroxylase (C).

Since cyanolysis of Se results in a loss of hydroxylase but not NADPH oxidase activity, we propose that Se functions in the early events in catalysis, namely, purine hydroxylation at the Mo site. We conclude that Se does not form part of an electron transfer chain because cyanolysis does not interrupt electron transfer between the cofactors using NADPH as a reductant. The lack of a selenium requirement for NADPH oxidase activity in PH, similar to that reported previously for NAH, lends further support to the conclusion that Se is a required cofactor for the forward hydroxylation reaction with purines. Although it appears that the labile Se cofactor is not structurally analogous to the cyanolyzable sulfur of XOR and AOR, it may be functioning in an analogous manner while coordinated to a cysteine sulfur. Interestingly, the high specific activity of PH (168 μmol min^{-1} mg^{-1}) in the optimized assay with hypoxanthine as substrate is similar to the activity of the selenium-dependent XDH from *C. barkeri* (164 μmol min^{-1} mg^{-1}, ref *4*). These turnover rates (greater than 400 s^{-1}) are significantly higher than those reported for non-selenium-dependent members of the family of molybdenum hydroxylases such as mammalian XOR (35 s^{-1}, ref *25*) and is indicative of a direct participation of the essential selenium cofactor in the hydroxylase reactions catalyzed by these bacterial molybdenum hydroxylases.

On the basis of the reported structures of various forms of Mop (*26*), diagrammed in Figure 10, we propose a structure of the molybdenum cofactor in selenium-dependent molybdenum hydroxylases (Figure 10C). We base this prediction on the similarity of the Mo(V) signal of hypoxanthine-reduced PH, the desulfo form of XOR, and the lack of hyperfine coupling of selenium to the Mo atom in ^{77}Se-enriched PH. While the structure of the selenium moiety has not been determined, its lability (cyanolysis) is most consistent with a perselenide derivative as shown in Figure 10C. Investigations using XAS are underway to identify the moiety of the selenium cofactor and ligands of Mo atom in PH, and the results of these studies should shed more light on understanding the role of selenium in catalysis in this unique class of selenoenzymes.

ACKNOWLEDGMENT

The authors would like to thank Prof. Hong In Lee (Kyungpook National University, Korea) for his initial EPR spectroscopy that led to this in-depth investigation. In addition, the authors would like to thank Matt Niebergal and Prof. John Lipscomb (University of Minnesota) for collecting several low temperature initial EPR datasets. We also thank Dr. Moon BinYim for use of the EPR laboratory at the NHLBI facility.

REFERENCES

1. Massey, V., and Harris, C. M. (1997) *Biochem. Soc. Trans. 25*, 750−755.
2. Hille, R. (1996) *Chem. Rev. 96*, 2757−2816.
3. Romao, M. J., Archer, M., Moura, I., Moura, J. J., LeGall, J., Engh, R., Schneider, M., Hof, P., and Huber, R. (1995) *Science 270*, 1170−1176.
4. Enroth, C., Eger, B. T., Okamoto, K., Nishino, T., Nishino, T., and Pai, E. F. (2000) *Proc. Natl. Acad. Sci. U.S.A. 97*, 10723−10728.
5. Bordas, J., Bray, R. C., Garner, C. D., Gutteridge, S., and Hasnain, S. S. (1980) *Biochem. J. 191*, 499−508.
6. Coughlan, M. P., and Rajagopalan, K. V. (1980) *Eur. J. Biochem. 105*, 81−84.
7. Massey, V., and Edmondson, D. (1970) *J. Biol. Chem. 245*, 6595−6598.
8. Wahl, R. C., Hageman, R. V., and Rajagopalan, K. V. (1984) *Arch. Biochem. Biophys. 230*, 264−273.
9. Dilworth, G. L. (1982) *Arch. Biochem. Biophys. 219*, 30−38.
10. Holcenberg, J. S., and Stadtman, E. R. (1969) *J. Biol. Chem. 244*, 1194−1203.
11. Schrader, T., Rienhofer, A., and Andreesen, J. R. (1999) *Eur. J. Biochem. 264*, 862−871.
12. Self, W. T., and Stadtman, T. C. (2000) *Proc. Natl. Acad. Sci. U.S.A. 97*, 7208−7213.
13. Wagner, R., and Andreesen, J. R. (1979) *Arch. Microbiol. 121*, 255−260.
14. Gladyshev, V. N., Khangulov, S. V., and Stadtman, T. C. (1994) *Proc. Natl. Acad. Sci. U.S.A. 91*, 232−236.
15. Gladyshev, V. N., Khangulov, S. V., and Stadtman, T. C. (1996) *Biochemistry 35*, 212−223.
16. Self, W. T. (2002) *J. Bacteriol. 184*, 2039−2044.
17. Hausinger, R. P., Honek, J. F., and Walsh, C. (1986) *Methods Enzymol. 122*, 199−209.
18. Gremer, L., and Meyer, O. (1996) *Eur. J. Biochem. 238*, 862−866.
19. Aasa, R., and Vänngard, T. (1975) *J. Magn. Reson. 19*, 308−315.
20. Poston, J. M., Stadtman, T. C., and Stadtman, E. R. (1971) *Methods Enzymol. 22*, 49−54.
21. Durre, P., Andersch, W., and Andreesen, J. R. (1981) *Int. J. Syst. Bacteriol. 31*, 184−194.
22. Durre, P., and Andreesen, J. R. (1982) *J. Gen. Microbiol. 128*, 1457−1466.
23. Caldeira, J., Belle, V., Asso, M., Guigliarelli, B., Moura, I., Moura, J. J., and Bertrand, P. (2000) *Biochemistry 39*, 2700−2707.
24. Rabinowitz, J. C., and Barker, H. A. (1956) *J. Biol. Chem. 218*, 161−174.
25. Olson, J. S., Ballou, D. P., Palmer, G., and Massey, V. (1974) *J. Biol. Chem. 249*, 4363−4382.
26. Huber, R., Hof, P., Duarte, R. O., Moura, J. J., Moura, I., Liu, M. Y., LeGall, J., Hille, R., Archer, M., and Romao, M. J. (1996) *Proc. Natl. Acad. Sci. U.S.A. 93*, 8846−8851.

BI030136K